

EPR studies of nitrogen-centred free radicals. Part 53.¹ Isolation, EPR spectra and magnetic characterization of *N*-(arylthio)-2,4-diaryl-6-cyanophenylaminyls

Masaaki Nakatsuji,^a Yozo Miura^{*a} and Yoshio Teki^b

^a Department of Applied Chemistry, Faculty of Engineering, Osaka City University, Sumiyoshi-ku, Osaka 558-8585, Japan

^b Department of Material Science, Graduate School of Science, Osaka City University, Sumiyoshi-ku, Osaka 558-8585, Japan

Received (in Cambridge, UK) 2nd January 2001, Accepted 9th March 2001

First published as an Advance Article on the web 9th April 2001

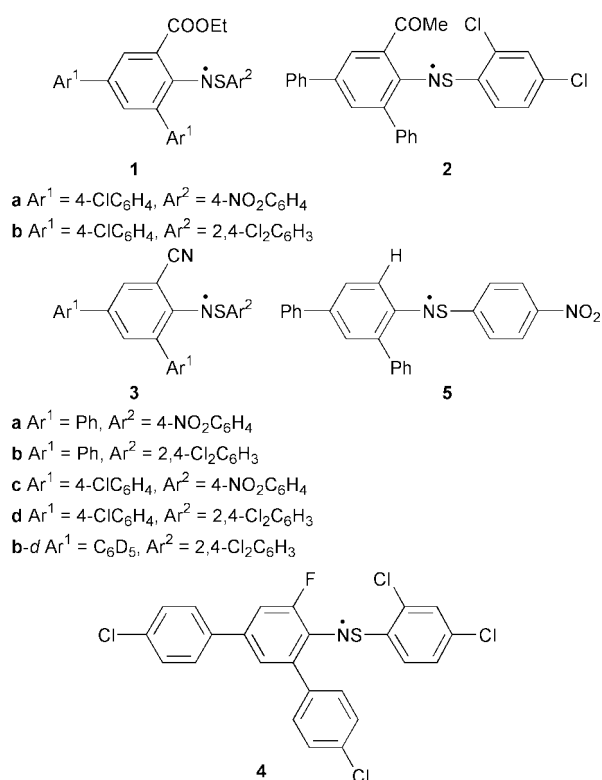
N-(Arylthio)-2,4-diaryl-6-ethoxycarbonylphenylaminyls (**1**), *N*-[(2,4-dichlorophenyl)thio]-2,4-diphenyl-6-acetylphenylaminyl (**2**), *N*-(arylthio)-2,4-diaryl-6-cyanophenylaminyls (**3**), *N*-[(2,4-dichlorophenyl)thio]-2,4-bis(4-chlorophenyl)-6-fluorophenylaminyl (**4**) and *N*-[(4-nitrophenyl)thio]-2,4-diphenylphenylaminyl (**5**) were generated by oxidation of the corresponding *N*-(arylthio)anilines. Although **4** and **5** were short-lived and decayed in 30 min, **1**–**3** were quite persistent and **3** could be isolated as radical crystals. EPR spectra were measured for all radicals generated and the spin density distribution was evaluated. *Ab initio* MO calculations (the UHF Becke 3LYP/STO 6-31G) were performed, and a quantitative discussion on the spin density distribution was made. Magnetic susceptibility measurements were performed for three isolated radicals with a SQUID magnetometer. One radical was found to couple ferromagnetically, and analysis with the one-dimensional regular Heisenberg model gave $2J/k_B = 11.2$ K.

Thioaminyl radicals are interesting as isolable nitrogen-centred free radicals.² This family of radicals, as well as cyclic NS radicals,³ are attractive spin sources for organic magnetism. Since thioaminyls have an extensively delocalized π -spin system, their magnetic interactions are expected to be strong compared with aminoxyl or imine *N*-oxide-aminoxyl radicals which have localized π -spin systems.^{4–6} In recent years we have designed isolable thioaminyl radicals. The isolated thioaminyls were subjected to magnetic measurements with a SQUID magnetometer, and it was found that six thioaminyls couple ferromagnetically.^{1,7–9} The magnetic interactions are 3.6–28 K ($2J/k_B$), which are much stronger than those of aminoxyl or imine *N*-oxide-aminoxyl radicals. In a continued study we investigated *o*-ethoxycarbonyl (**1**), acetyl (**2**), cyano (**3**) and fluoro (**4**) substituted thioaminyl radicals **1**–**4**, along with *ortho*-unsubstituted thioaminyl **5**. These thioaminyls are structurally interesting because we expected that these functional groups may strengthen the magnetic interactions between the radical molecules through the electrostatic interaction of functional groups. However, these radicals might not be sufficiently persistent to be isolated because the protection of the *ortho* position of the anilino benzene ring by the EtOCO, MeCO, or CN group seemed to be insufficient. Although radicals **4** and **5** did not persist for a long period, **1**–**3** were very long lived, and **3** could be isolated as radical crystals. Herein we report generation, isolation, EPR spectra, spin density calculations and magnetic properties of **3**, along with EPR spectra of **1**, **2**, **4** and **5**. Furthermore we report the decomposition mechanism of **4** and **5**.

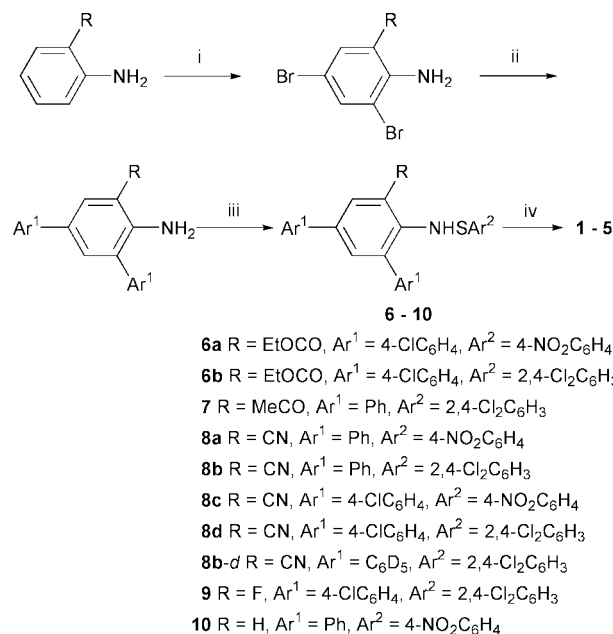
Results and discussion

Syntheses of precursors

The corresponding precursors **6**–**10** were prepared according to Scheme 1. Thus, treatment of 2-substituted anilines with benzyltrimethylammonium tribromide (BTMA Br₃)¹⁰ in CH₂Cl₂–MeOH in the presence of CaCO₃ gave the corresponding 2,4-



dibromo-6-*R*-anilines (*R* = OCOEt, COMe, CN, F) in 89–93% yields. The Pd-catalyzed cross-coupling reaction of 2,4-dibromo-6-*R*-anilines with arylboronic acid yielded 2,4-diaryl-6-*R*-anilines in 76–90% yields.¹¹ Preparation of 2,4-diaryl-aniline was previously reported by us.¹² Reaction of 2,6-diaryl-6-*R*-anilines or 2,4-diarylaniline with arenesulfonyl chlorides gave **6** in 40–48%, **7** in 42%, **8** in 36–52%, **9** in 52% and **10** in 48% yields, respectively. Precursors **6**–**8** and **10** were obtained as crystals, while **9** was a semi-solid.



Scheme 1 Reactions and conditions: i, BTMA Br₃, CaCO₃, CH₂Cl₂–MeOH, room temp; ii, Ar¹B(OH)₂, (PPh₃)₄Pd, K₂CO₃, benzene–EtOH–H₂O, reflux; iii, Ar²SCl, Et₃N, dry ether or THF, 0 °C; iv, PbO₂, benzene, room temp.

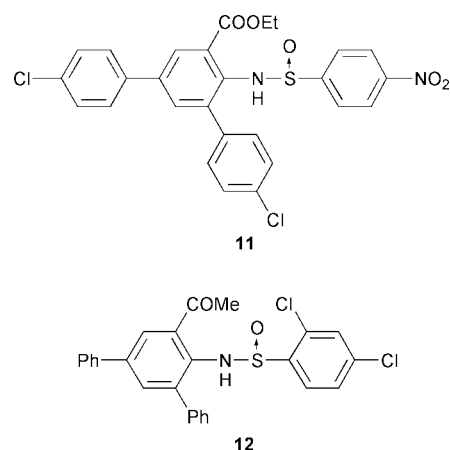
Generation and isolation of radicals

Oxidation of precursors **6–10** was carried out in benzene using PbO₂ as oxidant. When PbO₂ was added to stirred solutions of precursors, the solutions immediately turned to dark green. In the cases of **1–3** the characteristic green colours were almost constant for one day under the atmospheric conditions. However, when the solutions were left for a month at room temperature, the green colours completely disappeared (the half lifetimes, 1–3 weeks). In the case of **4** the dark green colour immediately disappeared and the solution turned dark brown. Thus, for measurements of EPR spectra, **4** was generated by the reaction of **9** and di-*tert*-butyl diperoxyoxalate. The diperoxy ester decomposes at a moderate rate at room temperature in hydrocarbon solvents such as benzene to give *tert*-butoxyl radicals.¹³ In the case of **5** the dark green colour was kept for 30 min, and the solution finally turned dark brown.

Isolation of **1–3** was tried by the following procedures. The corresponding precursors **6–8** were oxidized with PbO₂ and the reaction mixtures filtered. The solvent was removed by freeze-drying, and the resultant crystalline powder was crystallized. In the case of **3** all radicals examined (**3a–d**) were successfully isolated in 37–47% yields. On the other hand, isolation of **1** and **2** was unsuccessful in spite of much effort and only sulfonamides **11** and **12** were formed in 43 and 38% yields, respectively, in the oxidation of **6a** and **7**. Usually, sulfonamide is not formed in oxidation of precursors with PbO₂ and it is not clear why sulfonamide was formed in such a high yield in these cases. Removal of the sulfonamides by recrystallization or column chromatography was unsuccessful. Recrystallization gave a mixture of radical and sulfonamide, and column chromatography resulted in complete decomposition of radical. To suppress the formation of sulfonamides, oxidation was carried out in degassed benzene. However, formation of **11** or **12** was still observed, suggesting that the sulfonamide oxygen comes not from the atmospheric oxygen, but from PbO₂. Oxidation with Ag₂O was also attempted, but formation of **11** or **12** was still observed.

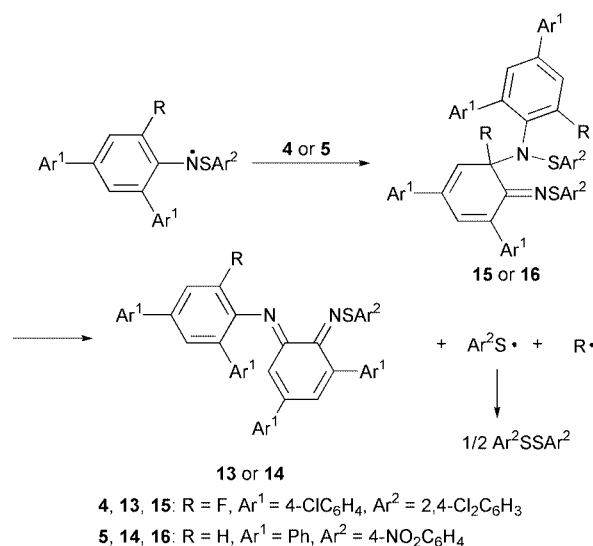
The mechanism for decomposition of **4** and **5**

In contrast to **1–3**, **4** and **5** were short-lived. The characteristic green colours disappeared immediately (**4**) or within 30 min (**5**). To clarify their decomposition mechanism, product analyses



were performed. Precursors **9** and **10** were oxidized with PbO₂ in benzene, and the mixtures were filtrated. The green-coloured solutions were allowed to stand until the green colour completely disappeared. After concentration, column chromatography of the solutions gave **13** and **14** in 41 and 38% yields, respectively. The structures of **13** and **14** were determined by IR, ¹H NMR, mass spectra and elemental analyses.

A plausible mechanism for the decomposition of **4** and **5** is depicted in Scheme 2.^{8,14–16} The first step is the N–C coupling



Scheme 2

between two thioaminy radicals to give **15** or **16**. Elimination of Ar²S• + F• from **15** yields **13**, and elimination of Ar²S• + H• from **16** yields **14**. If R is bulky enough to prevent the coupling reaction or if the C–R bond of the formed C–N coupled dimer is sufficiently strong, the radicals will be long lived like **1–3**. Thus, it is likely that the stabilities of this type of radical depend on the bulkiness of R and the bond strength of C–R.

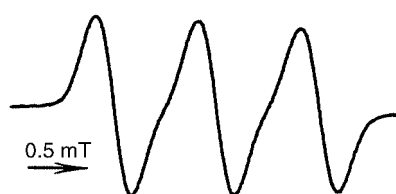
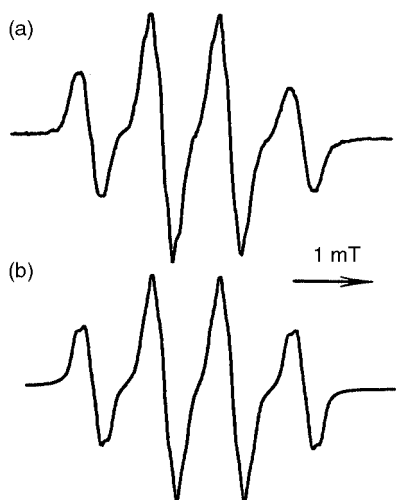
EPR spectra

EPR spectra of **1–5** were recorded at room temperature using benzene as solvent. A typical EPR spectrum is shown in Fig. 1 and EPR parameters are summarized in Table 1. Fig. 1 shows that the EPR spectrum of **3a** consists of a simple 1 : 1 : 1 triplet. Similar 1 : 1 : 1 triplet EPR spectra were observed for **1**, **2** and **3b–d**. The absence of proton hyperfine splittings is attributed to the presence of many protons with unresolved small hyperfine couplings (hfc). The peak-to-peak line widths (ΔH_{pp}) are therefore relatively large (0.283–0.316 mT). In the case of **4** an EPR spectrum (Fig. 2) was split into a 1 : 2 : 2 : 1 quartet by the interaction with a nitrogen atom and a fluorine atom. Computer simulation of this spectrum gave $a_N = 0.873$ and

Table 1 EPR parameters for **1–5** in benzene at 20 °C^a

Radical	a_N^b	a_{other}^c	g
1a	0.908		2.0059
1b	0.894		2.0058
2	0.907		2.0059
3a	0.851		2.0058
3b	0.847		2.0058
3c	0.844		2.0060
3d	0.853		2.0059
3b-d^d	0.853	0.130 (2H), ^e 0.085 (1H) ^f	2.0059
4^d	0.873	0.980 (1F)	2.0058
5^d	0.898	0.390 (1H) ^g	2.0061

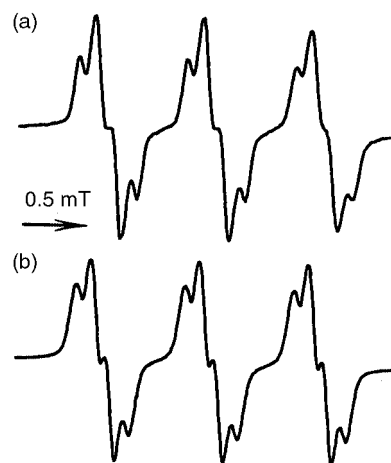
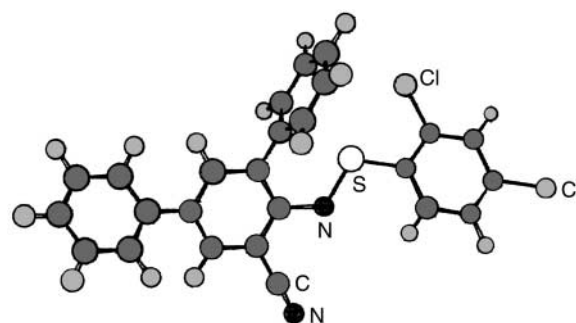
^a Hyperfine coupling (hfc) constants are given in mT. ^b The values for the NS nitrogen. ^c The number in parentheses refer to the number of equivalent H or F. ^d Hfc constants are determined by computer simulation. ^e The anilino *meta*-protons. ^f The arylthiyl *ortho*-proton. ^g The anilino *ortho*-proton.

**Fig. 1** The experimental EPR spectrum of **3a** in benzene at 20 °C.**Fig. 2** EPR spectrum of **4** in benzene at 20 °C. (a) Experimental; (b) simulation.

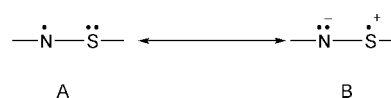
$a_F = 0.980$ mT. An EPR spectrum of **5** was split into doublets of a triplet by the interaction with a nitrogen and an anilino *ortho*-proton. Computer simulation of this spectrum gave $a_N = 0.898$ and $a_H = 0.390$ mT.

The 2- and 4-phenyl groups of **3b** were deuterated to detect hyperfine splittings due to protons. Such deuteration reduces the ΔH_{pp} of EPR spectra and this has often allowed the observation of hyperfine splittings due to protons. The precursor **8b-d** was prepared according to the same procedure as for the corresponding nondeuterated compound. An EPR spectrum of **3b-d** is shown in Fig. 3, along with a computer simulation. The spectrum is split into a 1 : 1 : 1 triplet, and each component of the triplet is further split into an incomplete 1 : 3 : 3 : 1 quartet. Computer simulation of the spectrum gave $a_N = 0.853$ and $a_H = 0.130$ (2H) and 0.085 mT (1H). The protons giving the hyperfine coupling constant of 0.130 mT are assigned to the anilino *meta*-protons and the proton giving the hfs constant of 0.085 mT to the phenylthiyl *ortho*-proton.

When the hfc constants are compared to each other, one may note that the a_N values of **3** (0.844–0.853 mT) are ~0.05 mT

**Fig. 3** EPR spectrum of **3b-d** in benzene at 20 °C. (a) Experimental; (b) simulation.**Fig. 4** Optimized structure of **3b** calculated by the MNDO/AM1 method.

lower than those of the others (0.873–0.908 mT). If this decrease in a_N is explained in terms of an enhancement of canonical form B (Scheme 3) due to an electron-withdrawing

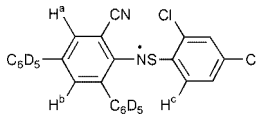
**Scheme 3**

CN group, an increase in g must also be observed. However, such an increase in g is not observed for any radicals **3**. Therefore, an enhancement of canonical form B can be ruled out. An alternative explanation is a delocalization of the unpaired electron spin onto CN. The *ab initio* calculations predict a considerable delocalization of the unpaired electron spin onto CN as described below. Since the a_N values for **1** and **2** are very similar to that of **5**, we assume that the EtOCO and COMe groups are significantly twisted from the anilino benzene ring.

Spin density calculations

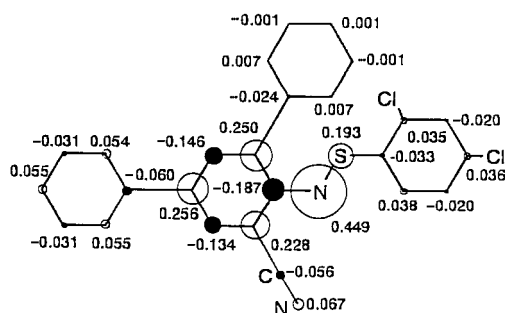
The spin density distribution in **3b** was calculated by the *ab initio* molecular orbital (MO) calculations based on density functional theory. The electronic structure of the radical molecule was calculated using Gaussian 98.¹⁷ The molecular structure was optimized by the semi-empirical MO calculations (MNDO/AM1 method). The *ab initio* calculations were carried out using the STO 6-31G basis sets and the UHF Becke 3LYP hybrid method. The optimized geometry is shown in Fig. 4 and the calculated spin densities are shown in Fig. 5. In Table 2, the calculated and experimental hfc constants are compared.

Fig. 4 shows that the ArN–SAr π -framework is almost planar, and the benzene ring at the *para* position makes a twisted angle of 32° with the anilino benzene ring. On the other hand, the benzene ring at the *ortho* position makes a twisted

Table 2 Experimental and calculated hyperfine coupling constants of **3d-d**


Atom	Experimental $ a_x /\text{mT}$	Calculation a_x^a/mT
N ^c	0.853	1.088
H ^a	0.130	0.247
H ^b	0.130	0.274
H ^c	0.085	-0.086

^a The values calculated for **3b**. ^b The calculations were performed by the *ab initio* method at the UHF B3LYP/STO 6-31G level. ^c The value for the NS nitrogen.

**Fig. 5** Total atomic spin densities for **3b** calculated by the UHF Becke 3LYP hybrid method using the STO 6-31G basis set.

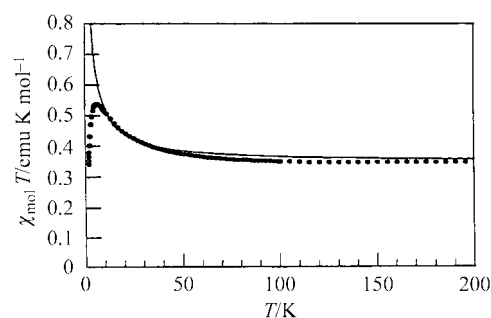
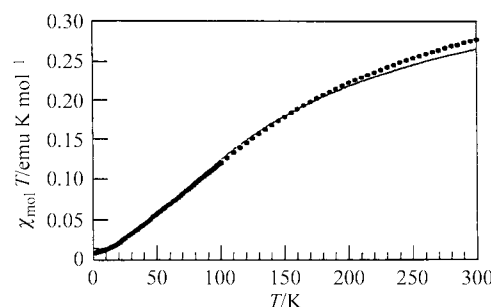
angle of 89° due to the steric congestion around the radical centre. Such an optimized structure is common for thioaminy radicals, as clarified by X-ray crystallographic analyses.^{1,8,9} Since it was previously confirmed that the structures of thioaminy radicals optimized by the above calculation method are in excellent agreement with those determined by X-ray crystallography,¹ we believe that the present calculations yield a reliable structure.

Although the calculations give somewhat large hfc constants for N, as well as the anilino *meta*-protons, good agreements between the observed hfc constants and the calculations are found (see Table 2). Fig. 5 shows that the unpaired electron spin is extensively delocalized over the whole of the radical molecule, with the particularly high spin densities on the NS and anilino benzene ring. We also note that there is some spin density on the cyano group. This is in accordance with the above explanation for a decrease in a_N of **3**.

Magnetic susceptibility measurements

The magnetic susceptibility (χ_{mol}) measurements were performed for the isolated four radicals using polycrystalline samples with a SQUID magnetometer in the temperature range 1.8–300 K. The diamagnetic corrections were made based on Pascal's sum rule. The spin concentrations of the radical samples used were >95% as determined by EPR.

Fig. 6 shows $\chi_{\text{mol}}T$ vs. T plots for **3a**. The $\chi_{\text{mol}}T$ value is constant (0.376 emu K mol⁻¹) above 100 K and increases with decreasing temperature below 100 K. It then reaches a maximum of 0.54 emu K mol⁻¹ at 6 K and decreases with decreasing temperature. When the magnetic behaviour was analyzed by the modified Bleaney–Bower model, no satisfactory agreement with the experimental data was obtained. On the other hand, analysis with the one-dimensional regular Heisenberg model¹⁸ [when $\theta = 0$ K in eqn. (1)] gave a satisfactory agreement with the experimental data in the temperature region of 50–300 K, and $2J/k_B$ was determined to be +11.2 K. However, when $\theta = -2, -5, -10$ and -15 K, no satisfactory agreement with the experimental data was obtained. Although

**Fig. 6** $\chi_{\text{mol}}T$ vs. T plots of **3a**. The solid line was calculated by the one-dimensional Heisenberg model.**Fig. 7** $\chi_{\text{mol}}T$ vs. T plots of **3b**. The solid line was calculated by the one-dimensional alternating model.

it is obvious that the intrachain interaction is ferromagnetic and the interchain interaction is antiferromagnetic, we could not reconstruct the experimental data by eqn. (1).

$$H = -2J \frac{T}{T - \theta} \sum S_i S_j \quad (1)$$

Radical **3b** showed a strong antiferromagnetic interaction. As found in Fig. 7, the $\chi_{\text{mol}}T$ value at 300 K is already lower than the Curie constant of 0.376 emu K mol⁻¹ for the $S = \frac{1}{2}$ systems, and it was drastically decreased with decreasing temperature and became nearly 0 emu K mol⁻¹ at 2 K. Such a magnetic behaviour indicates a strong antiferromagnetic interaction between the radical molecules, and this suggests that there is a large SOMO–SOMO overlap between the neighbouring radical molecules. The best fit with the experimental data with the alternating linear chain model¹⁹ [eqn. (2)] gave $2J/k_B = -200$ K and a (alternating parameter) = 0.87.

$$H = -2J \sum (S_{2i-1} S_{2i} + a S_{2i} S_{2i+1}) \quad (2)$$

Antiferromagnetic interaction was also observed for **3d**. The $\chi_{\text{mol}}T$ vs. T plots were analyzed with the dimer model, and the intra-dimer interaction was determined to be $2J/k_B = -56.8$ K. In the case of **3c**, the magnetic interaction was very weak and the presence of a large number of lattice defects was indicated in the SQUID magnetometer. Thus, a reliable analysis of the experimental data was impossible.

Conclusions

Four kinds of *N*-(arylthio)-2,4-diaryl-6-*R*-phenylaminyls ($R = \text{EtOCO}, \text{MeCO}, \text{CN}, \text{F}$) and *N*-[(4-nitrophenyl)thio]-2,4-diphenylphenylaminyl were generated. EtOCO-, MeCO- and CN-substituted radicals were long-lived, and CN-substituted radicals were isolated as radical crystals. F-substituted and unsubstituted radicals were short-lived and their decomposition mechanism was elucidated based on the product analyses. The EPR spectra and *ab initio* MO calculations (UHF Becke 3LYP/STO 6-31G) showed an extensive delocalization over the whole of the radical molecule. Magnetic susceptibility

measurements were performed for three isolated radicals. One radical (**3a**) showed a ferromagnetic interaction and the $\chi_{\text{mol}}T$ vs. T plots by the one-dimensional regular Heisenberg model gave $2J/k_B = +11.2$ K. The other two radicals showed an anti-ferromagnetic interaction. Analyses of the $\chi_{\text{mol}}T$ vs. T plots with the alternating linear chain model (**3b**) or the dimer model (**3d**) gave $2J/k_B = -200$ K and $a = 0.87$ (**3b**) and $2J/k_B = -56.8$ K (**3d**), respectively.

Experimental

Melting points were determined with a Yanagimoto micro melting point apparatus and are uncorrected. IR spectra were obtained on a JASCO FT/IR-230 spectrophotometer. UV-Vis spectra were recorded on a Shimadzu UV-2200 spectrophotometer. ^1H NMR spectra were measured with a JEOL α -400 spectrometer (400 MHz); chemical shifts are expressed in ppm (δ) using tetramethylsilane as an internal standard and J values are given in Hz. EPR spectra were measured with a Bruker ESP-300 spectrometer equipped with a X-band microwave unit and with a 100 kHz field modulation. The hyperfine coupling constants and g values were determined by measurement of Fremy's salt in a dilute K_2CO_3 aqueous solution ($a_N = 1.309$ mT; $g = 2.0057$) as the reference. Mass spectra (FAB) were measured by a JEOL JX-700T mass spectrometer. Magnetic susceptibility measurements were carried out with a Quantum Design SQUID magnetometer MPMS2 in the 1.8–300 K temperature range. The diamagnetic contributions of samples were estimated from the Pascal diamagnetic constants. Silica gel column chromatography was carried out on Fuji silysia BW-127ZH (Fuji-Davison chem.) and alumina column chromatography on Merck aluminium oxide 90.

Bromination of 2-ethoxycarbonyl-, 2-acetyl-, 2-cyano- and 2-fluoroanilines were carried out by treating 2-substituted anilines (40 mmol) with benzyltrimethylammonium tribromide¹⁰ (BTMA Br₃) (39.0 g, 100 mmol) in CH_2Cl_2 (250 cm³)–MeOH (100 cm³) at room temperature for 1 h in the presence of CaCO_3 (11.2 g). The usual workup and crystallization (EtOH) gave 2-(ethoxycarbonyl)-4,6-dibromoaniline (colourless needles; mp 72–74 °C) in 89%, 2-acetyl-4,6-dibromoaniline (yellow needles, mp 129–131 °C) in 93%, 2-cyano-4,6-dibromoaniline (colourless needles, mp 156–158 °C) in 92%, and 2-fluoro-4,6-dibromoaniline (colourless needles, mp 60–63 °C) in 89% yields. (Phenyl- d_5)boronic acid was obtained by the reported method.²⁰ 2,4-Diphenylaniline was obtained by our previous method.¹² Di-*tert*-butyl diperoxyoxalate was obtained by the reported method.¹³

General procedure for preparation of 2,4-diaryl-6-R-anilines (R = COOEt, COMe, CN and F)

A mixture of 2-R-4,6-dibromoanilines (25 mmol), arylboronic acid (75 mmol), $(\text{PPh}_3)_4\text{Pd}$ (1.73 g, 1.50 mmol) and K_2CO_3 (27.6 g) in benzene (250 cm³)–EtOH (50 cm³)– H_2O (100 cm³) was refluxed for 15 h under a nitrogen atmosphere.^{11,12} The organic layer was extracted, washed with brine, dried (MgSO_4), and concentrated under reduced pressure. The residue was then chromatographed on silica gel with 1 : 5 hexane–benzene [2,4-bis(4-chlorophenyl)-6-fluoroaniline], CH_2Cl_2 [2,4-bis(4-chlorophenyl)-2-cyanoaniline] or benzene (the other anilines) and crystallized from appropriate solvents.

2,4-Bis(4-chlorophenyl)-6-ethoxycarbonylaniline. Colourless needles (EtOH); yield 90%; mp 120–122 °C; ν (KBr)/cm^{−1} 3480 and 3360 (NH₂), 1690 (C=O); δ_{H} (CDCl₃) 1.42 (t, J 7.0, CH₃, 3H), 4.38 (q, J 7.0, CH₂, 2H), 6.02 (br s, NH₂, 2H), 7.35–7.50 (m, ArH, 9H), 8.14 (d, J 2.0, ArH, 1H) (Found: C, 65.25; H, 4.38; N, 3.55. C₂₁H₁₇Cl₂NO₂ requires: C, 65.30; H, 4.44; N, 3.63%).

2,4-Diphenyl-6-acetylaniline. Yellow prisms (EtOH); yield 79%; mp 68–70 °C; ν (KBr)/cm^{−1} 3480 and 3320 (NH₂), 1650 (C=O); δ_{H} (CDCl₃) 2.70 (s, Me, 3H), 6.62 (br s, NH₂, 2H), 7.30 (t, J 7.3, ArH, 1H), 7.38–7.58 (m, ArH, 10H), 7.97 (d, J 2.4, ArH, 1H) (Found: C, 83.53; H, 5.91; N, 4.81. C₂₀H₁₇NO requires: C, 83.59; H, 5.96; N, 4.87%).

2,4-Diphenyl-6-cyanoaniline. Colourless prisms (EtOH); yield 83%; mp 88–90 °C; ν (KBr)/cm^{−1} 3470, 3440, 3370 and 3340 (NH₂), 2220 (CN); δ_{H} (CDCl₃) 4.57 (br s, NH₂, 2H), 7.32 (t, J 7.8, ArH, 1H), 7.34–7.55 (m, ArH, 10H), 7.65 (d, J 2.4, ArH, 1H) (Found: C, 84.26; H, 5.17; N, 10.23. C₁₉H₁₄N₂ requires: C, 84.42; H, 5.22; N, 10.36%).

2,4-Bis(4-chlorophenyl)-6-cyanoaniline. Colourless prisms (EtOH); yield 79%; mp 126–128 °C; ν (KBr)/cm^{−1} 3480 and 3390 (NH₂), 2220 (CN); δ_{H} (CDCl₃) 4.56 (s, NH₂, 2H), 7.37–7.50 (m, ArH, 9H), 7.61 (d, J 2.4, ArH, 1H) (Found: C, 67.02; H, 3.61; N, 8.09. C₁₉H₁₂Cl₂N₂ requires: C, 67.27; H, 3.57; N, 8.26%).

2,4-Di(phenyl- d_5)-6-cyanoaniline. Colourless prisms (EtOH); yield 76%; mp 91–93 °C; ν (KBr)/cm^{−1} 3470, 3440, 3370 and 3330 (NH₂), 2220 (CN); δ_{H} (CDCl₃) 4.57 (s, NH₂, 2H), 7.55 (d, J 2.4, ArH, 1H), 7.64 (d, J 2.4, ArH, 1H) (Found: C, 81.26; H, 5.07; N, 9.85. C₂₁H₄D₁₀N₂ requires: C, 81.39; H, 5.03; N, 9.99%).

2,4-Bis(4-chlorophenyl)-6-fluoroaniline. Brown needles (EtOH); yield 83%; mp 97–99 °C; ν (KBr)/cm^{−1} 3440 and 3300 (NH₂); δ_{H} (CDCl₃) 3.88 (s, NH₂, 2H), 7.12 (d, J 2.4, ArH, 1H), 7.35–7.49 (m, ArH, 9H) (Found: C, 65.24; H, 3.87; N, 3.99. C₁₈H₁₂Cl₂FN requires: C, 65.08; H, 3.64; N, 4.22%).

General procedure for preparation of *N*-(arythio)-2,4-diaryl-6-R-anilines (R = COOEt, COMe, CN and F)

To a stirred solution of 2,4-diaryl-6-R-anilines (6.30 mmol) and Et₃N (1.46 g, 14.43 mmol) in dry ether (or anhydrous THF) (200 cm³), was added at 0 °C a solution of arenesulfonyl chloride (7.8 mmol) in dry ether (or anhydrous THF) (20 cm³). After being stirred for 2 h at 0 °C, the mixture was filtered and concentrated under reduced pressure, and the residue was chromatographed on alumina with 1 : 5 benzene–hexane (**9**), 1 : 1 benzene–hexane (**6b**, **7**, **8b**, **8d**, **8b-d**), or 1 : 2 hexane–benzene (**6a**, **8a**, **8c**, **10**) and crystallized from appropriate solvents. Compound **9** was obtained as an oil.

***N*[(4-Nitrophenyl)thio]-2,4-bis(4-chlorophenyl)-6-ethoxycarbonylaniline 6a.** Light yellow needles (EtOH–benzene); yield 48%; mp 179–181 °C; ν (KBr)/cm^{−1} 3240 (NH), 1680 (C=O); δ_{H} (CDCl₃) 1.41 (t, J 6.8, CH₃, 3H), 4.39 (q, J 6.8, CH₂, 2H), 7.44–7.55 (m, ArH, 8H), 7.66 (d, J 2.4, ArH, 1H), 7.68 (d, J 8.8, ArH, 2H), 8.33 (d, J 2.0, ArH, 1H), 8.42 (d, J 8.8, ArH, 2H), 9.64 (s, NH, 1H) (Found: C, 60.14; H, 3.79; N, 5.13. C₂₇H₂₀Cl₂N₂O₄S requires: C, 60.12; H, 3.74; N, 5.19%).

***N*[(2,4-Dichlorophenyl)thio]-2,4-bis(4-chlorophenyl)-6-ethoxycarbonylaniline 6b.** Colourless prisms (EtOH); yield 40%; mp 89–91 °C; ν (KBr)/cm^{−1} 3260 (NH), 1680 (C=O); δ_{H} (CDCl₃) 1.46 (t, J 7.2, CH₃, 3H), 4.45 (q, J 7.2, CH₂, 2H), 7.09–7.12 (m, ArH, 3H), 7.15–7.23 (m, ArH, 3H), 7.38–7.50 (m, ArH, 6H), 8.15 (d, J 2.4, ArH, 1H), 8.85 (s, NH, 1H) (Found: C, 57.89; H, 3.32; N, 2.40. C₂₇H₁₉Cl₄NO₂S requires: C, 57.57; H, 3.40; N, 2.49%).

***N*[(2,4-Dichlorophenyl)thio]-2,4-diphenyl-6-acetylaniline 7.** Yellow plates (EtOH); yield 42%; mp 136–138 °C; ν (KBr)/cm^{−1} 3240 (NH), 1650 (C=O); δ_{H} (CDCl₃) 2.77 (s, Me, 3H), 7.04–7.57 (m, ArH, 14H), 7.97 (d, J 2.4, ArH, 1H), 9.29 (s, NH, 1H)

(Found: C, 67.34; H, 4.35; N, 3.06. $C_{26}H_{19}Cl_2NOS$ requires: C, 67.24; H, 4.12; N, 3.02%).

***N*–[(4-Nitrophenyl)thio]–2,4-diphenyl-6-cyanoaniline 8a.** Yellow needles (EtOH–benzene); yield 37%; mp 173–175 °C; ν (KBr)/ cm^{-1} 3370 (NH), 2220 (CN); δ_H (CDCl₃) 5.72 (s, NH, 1H), 7.32–7.62 (m, ArH, 13H), 7.82 (d, *J* 2.4, ArH, 1H), 8.17 (d, *J* 8.8, ArH, 2H) (Found: C, 70.98; H, 4.04; N, 9.91. $C_{25}H_{17}N_3O_2S$ requires: C, 70.90; H, 4.05; N, 9.92%).

***N*–[(2,4-Dichlorophenyl)thio]–2,4-diphenyl-6-cyanoaniline 8b.** Colourless prisms (EtOH); yield 52%; mp 127–129 °C; ν (KBr)/ cm^{-1} 3350 (NH), 2220 (CN); δ_H (CDCl₃) 5.62 (s, NH, 1H), 7.13–7.57 (m, ArH, 14H), 7.81 (d, *J* 2.5, ArH, 1H) (Found: C, 67.33; H, 3.36; N, 6.46. $C_{25}H_{16}Cl_2N_2S$ requires: C, 67.11; H, 3.60; N, 6.26%).

***N*–[(4-Nitrophenyl)thio]–2,4-bis(4-chlorophenyl)-6-cyanoaniline 8c.** Yellow prisms (EtOH–benzene); yield 39%; mp 193–195 °C; ν (KBr)/ cm^{-1} 3370 (NH), 2230 (CN); δ_H (CDCl₃) 5.65 (s, NH, 1H), 7.30–7.50 (m, ArH, 10H), 7.53 (d, *J* 2.0, ArH, 1H), 7.78 (d, *J* 2.0, ArH, 1H), 8.17 (d, *J* 8.8, ArH, 2H) (Found: C, 61.11; H, 3.25; N, 8.69. $C_{25}H_{15}Cl_2N_3O_2S$ requires: C, 60.98; H, 3.07; N, 8.53%).

***N*–[(2,4-Dichlorophenyl)thio]–2,4-bis(4-chlorophenyl)-6-cyanoaniline 8d.** Colourless prisms (EtOH); yield 47%; mp 108–110 °C; ν (KBr)/ cm^{-1} 3370 (NH), 2230 (CN); δ_H (CDCl₃) 5.56 (s, NH, 1H), 7.01–7.32 (m, ArH, 4H), 7.40–7.76 (m, ArH, 7H), 7.48 (d, *J* 2.4, ArH, 1H), 7.75 (d, *J* 2.4, ArH, 1H) (Found: C, 58.17; H, 2.57; N, 5.21. $C_{25}H_{14}Cl_4N_2S$ requires: C, 58.16; H, 2.73; N, 5.43%).

***N*–[(2,4-Dichlorophenyl)thio]–2,4-di(phenyl-*d*₅)-6-cyanoaniline 8b-*d*.** Colourless needles (EtOH); yield 36%; mp 141–143 °C; ν (KBr)/ cm^{-1} 3270 (NH), 2230 (CN); δ_H (CDCl₃) 5.62 (s, NH, 1H), 7.21 (dd, *J* 8.3 and 2.0, ArH, 1H), 7.30 (d, *J* 2.0, ArH, 1H), 7.31 (d, *J* 8.3, ArH, 1H), 7.57 (d, *J* 2.0, ArH, 1H), 7.81 (d, *J* 2.0, ArH, 1H) (Found: C, 65.88; H, 3.62; N, 6.18. $C_{25}H_6D_{10}Cl_2N_2S$ requires: C, 65.64; H, 3.53; N, 6.12%).

***N*–[(2,4-Dichlorophenyl)thio]–2,4-bis(4-chlorophenyl)-6-fluoroaniline 9.** Brown semi-solid; yield 52%; ν (KBr)/ cm^{-1} 3300 (NH); δ_H (CDCl₃) 5.49 (s, NH, 1H), 7.17 (dd, *J* 8.4 and 1.9, ArH, 1H), 7.24 (d, *J* 1.9, ArH, 1H), 7.27–7.40 (m, ArH, 10H), 7.56 (d, *J* 8.4, ArH, 1H); *m/z* (FAB) 506.9598 ($C_{24}H_{14}Cl_4FNS$ requires: 506.9585).

***N*–[(4-Nitrophenyl)thio]–2,4-diphenylaniline 10.** Yellow needles (EtOH–benzene); yield 48%; mp 130–132 °C; ν (KBr)/ cm^{-1} 3410 and 3380 (NH); δ_H (CDCl₃) 5.49 (s, NH, 1H), 7.29–7.57 (m, ArH, 15H), 8.16 (d, *J* 8.8, ArH, 2H) (Found: C, 71.98; H, 4.43; N, 7.03. $C_{24}H_{18}N_2O_2S$ requires: C, 72.34; H, 4.55; N, 7.03%).

Isolation of *N*–(arylthio)–2,4-diphenyl-6-cyanophenylaminyls

Precursor **8** (100 mg) was dissolved in benzene (20 cm³) and K₂CO₃ (2–3 g) was added, and the resulting mixture was vigorously stirred. PbO₂ (2.0–3.0 g) was then added in several portions during 2.0 min and stirring was continued for an additional 0.5–1.0 min. The dark green mixture was filtered, the solvent was removed by freeze-drying, and the resulting dark green crystalline residue was crystallized from EtOH–EtOAc.

***N*–[(4-Nitrophenyl)thio]–2,4-diphenyl-6-cyanophenylaminyl 3a.** Dark green needles; yield 47%; mp 123–125 °C; λ_{max} (benzene)/nm 658 ($\epsilon/dm^3 mol^{-1}$ cm^{–1} 12100), 485 (6400sh), 406 (19200 ϵ_{max}), 375 (15200sh), 338 (10700sh); ν (KBr)/ cm^{-1} 3300,

2220, 1570, 1520, 1340, 860, 700 (Found: C, 71.23; H, 4.00; N, 10.05. $C_{25}H_{16}N_3O_2S$ requires: C, 71.07; H, 3.82; N, 9.95%).

***N*–[(2,4-Dichlorophenyl)thio]–2,4-diphenyl-6-cyanophenylaminyl 3b.** Dark green needles; yield 37%; mp 111–113 °C; λ_{max} (benzene)/nm 668 ($\epsilon/dm^3 mol^{-1}$ cm^{–1} 11800), 450 (4400sh), 386 (25300 ϵ_{max}), 370 (20700sh); ν (KBr)/ cm^{-1} 2920, 2850, 2210, 1740, 1570, 1460, 760, 690 (Found: C, 67.05; H, 3.56; N, 6.13. $C_{25}H_{15}Cl_2N_2S$ requires: C, 67.27; H, 3.39; N, 6.28%).

***N*–[(4-Nitrophenyl)thio]–2,4-bis(4-chlorophenyl)-6-cyanophenylaminyl 3c.** Dark green needles; yield 41%; mp 151–153 °C; λ_{max} (benzene)/nm 667 ($\epsilon/dm^3 mol^{-1}$ cm^{–1} 6700), 480 (4700sh), 412 (17700 ϵ_{max}), 375 (13700sh); ν (KBr)/ cm^{-1} 3100, 2920, 2200, 1580, 1520, 1340, 1100, 1010, 860, 820, 740 (Found: C, 61.25; H, 2.72; N, 8.66. $C_{25}H_{14}Cl_2N_3O_2S$ requires: C, 61.11; H, 2.87; N, 8.55%).

***N*–[(2,4-Dichlorophenyl)thio]–2,4-bis(4-chlorophenyl)-6-cyanophenylaminyl 3d.** Dark green needles; yield 39%; mp 133–135 °C; λ_{max} (benzene)/nm 673 ($\epsilon/dm^3 mol^{-1}$ cm^{–1} 9600), 472 (4800sh), 392 (19300 ϵ_{max}), 370 (16500sh), 331 (11200sh); ν (KBr)/ cm^{-1} 3080, 2920, 2210, 1570, 1490, 1440, 1090, 1020, 820 (Found: C, 58.17; H, 2.57; N, 5.21. $C_{25}H_{13}Cl_4N_2S$ requires: C, 58.27; H, 2.54; N, 5.44%).

Isolation and identification of 11

Precursor **6a** (100 mg, 0.180 mmol) was dissolved in 10 cm³ of benzene with stirring. After 1.0 g of K₂CO₃ was added, 2.0 g of PbO₂ was added in several portions during 2.0 min and the resulting mixture was further stirred for 0.5 min. After filtration, the filtrate was evaporated and the residue was chromatographed on alumina with 1 : 1 benzene–hexane to give **11** in 43% yield. Recrystallization from hexane gave colourless needles. Mp 138 °C (decomp.); *m/z* 553 ($M^+ - 1$, 100); ν (KBr)/ cm^{-1} 3190 (NH), 1710 (C=O), 1240 (SO); δ_H (CDCl₃) 1.37 (t, *J* 7.3, CH₃, 3H), 4.45 (q, *J* 7.3, CH₂, 2H), 7.42–7.44 (m, ArH, 8H), 7.50 (d, *J* 8.8, ArH, 2H), 7.57 (d, *J* 2.0, ArH, 1H), 8.19 (d, *J* 8.8, ArH, 2H), 8.22 (d, *J* 2.0, ArH, 1H), 9.64 (s, NH, 1H) (Found: C, 58.37; H, 3.86; N, 4.87. $C_{27}H_{20}Cl_2N_2O_5S$ requires: C, 58.39; H, 3.63; N, 5.04%).

Isolation and identification of 12

Precursor **7** (200 mg, 0.43 mmol) was dissolved in 10 cm³ of benzene with stirring. After 2.0 g of K₂CO₃ was added, 6.0 g of PbO₂ was added in several portions during 2.0 min and the resulting mixture was further stirred for 1 min. After filtration, the filtrate was evaporated and the residue was chromatographed on alumina with benzene to give **12** in 38%. Recrystallization from hexane–benzene gave brown prisms. Mp 58–60 °C; *m/z* 479 ($M^+ - 1$, 100); ν (KBr)/ cm^{-1} 3480 (NH), 1650 (C=O), 1240 (SO); δ_H (CDCl₃) 2.71 (s, CH₃, 3H), 7.29 (d, *J* 2.0, ArH, 1H), 7.39–7.49 (m, ArH, 7H), 7.55–7.60 (m, ArH, 4H), 7.67 (d, *J* 2.0, ArH, 1H), 7.82 (d, *J* 2.0, ArH, 1H), 8.03 (d, *J* 2.0, ArH, 1H), 10.37 (s, NH, 1H) (Found: C, 65.21; H, 4.11; N, 3.05. $C_{26}H_{19}Cl_2NO_2S$ requires: C, 65.00; H, 3.99; N, 2.92%).

Product analysis for decomposition of 4

Precursor **9** (100 mg, 0.20 mmol) was dissolved in 10 cm³ of benzene with stirring. After 1.0 g of K₂CO₃ was added, 2.0 g of PbO₂ was added in several portions during 2.0 min and the resulting mixture was further stirred for 0.5 min. After filtration, the brown filtrate was evaporated and the residue was chromatographed on alumina with 1 : 9 benzene–hexane to give **13** as a dark brown solid in 41% yield. Recrystallization from EtOH gave brown needles with mp >300 °C; *m/z* (FAB) 816 (M^+); δ_H (CDCl₃) 6.66 (d, *J* 2.0, ArH, 1H), 7.01 (d, *J* 2.0, ArH,

1H), 7.13 (dd, *J* 8.8 and 2.0, ArH, 1H), 7.28 (d, *J* 8.8, ArH, 2H), 7.31 (d, *J* 2.0, ArH, 1H), 7.36–7.50 (m, ArH, 15H), 7.59 (d, *J* 8.8, ArH, 2H) (Found: C, 61.66; H, 2.71; N, 3.39. C₄₂H₂₃Cl₆FN₂S requires: C, 61.56; H, 2.83; N, 3.42%).

Product analysis for decomposition of **5**

Precursor **10** (100 mg, 0.25 mmol) was dissolved in 10 cm³ of benzene with stirring. After 1.0 g of K₂CO₃ was added, 2.0 g of PbO₂ was added in several portions during 2.0 min and the resulting mixture was further stirred for 0.5 min. After filtration, the filtrate was evaporated and the residue was chromatographed on alumina with 1 : 1 benzene–hexane to give **14** as a dark brown solid in 38% yield. Recrystallization from EtOH gave brown needles with mp 191–193 °C; *m/z* (FAB) 640 (M⁺ + 1); δ_H (CDCl₃) 6.93 (d, *J* 2.4, ArH, 1H), 7.11–7.13 (m, ArH, 2H), 7.21–7.59 (m, ArH, 20H), 7.67–7.72 (m, ArH, 3H), 7.79 (d, *J* 2.4, ArH, 1H), 8.76 (d, *J* 9.3, ArH, 2H) (Found: C, 78.66; H, 4.57; N, 6.46. C₄₂H₂₉N₃O₂S requires: C, 78.85; H, 4.57; N, 6.57%).

References

- 1 Part 52. Y. Miura, T. Tomimura and Y. Teki, *J. Org. Chem.*, 2000, **65**, 7889.
- 2 Y. Miura in *Recent Research Developments in Organic Chemistry*, Transworld Research Network, India, 1998, vol. 2, part II, p. 251.
- 3 J. M. Farrar, M. K. Patel, P. Kaszynski and V. G. Young, *J. Org. Chem.*, 2000, **65**, 931; G. D. McManus, J. M. Rawson, N. Feeder, F. Palacio and P. Oliete, *J. Mater. Chem.*, 2000, **10**, 2001; T. M. Barclay, A. W. Cordes, R. C. Haddon, M. E. Itkis, R. T. Oakley, R. W. Reed and H. Zhang, *J. Am. Chem. Soc.*, 1999, **121**, 969, and references cited therein.
- 4 A. R. Forrester, J. M. Hay and H. R. Thomson, *Organic Chemistry of Stable Free Radicals*, Academic Press, London and New York, 1968; E. G. Rozantsev, *Free Nitroxyl Radicals*, Plenum Press, New York and London, 1970; L. B. Volodarsky, V. A. Reznikov and V. I. Ovcharenko, *Synthetic Chemistry of Stable Nitroxides*, CRC Press, Boca Raton, 1994.
- 5 *Magnetic Properties of Organic Materials*, ed P. M. Lahti, Marcel Dekker, New York, 1999.
- 6 Proceedings of the 5th International Conference on Molecule-Based Magnets, *Mol. Cryst. Liq. Cryst.*, 1999, **334**, 1 and **335**, 1.
- 7 Y. Teki, K. Itoh, A. Okada, H. Yamakage, T. Kobayashi, K. Amaya, S. Kurokawa, S. Ueno and Y. Miura, *Chem. Phys. Lett.*, 1997, **270**, 573.
- 8 Y. Miura, M. Momoki, M. Nakatsuji and Y. Teki, *J. Org. Chem.*, 1998, **63**, 1555.
- 9 Y. Miura, S. Kurokawa, M. Nakatsuji, K. Ando and Y. Teki, *J. Org. Chem.*, 1998, **63**, 8295.
- 10 S. Kajigaeshi, T. Kakinami, K. Inoue, M. Kondo, H. Nakamura, M. Fujikawa and T. Okamoto, *Bull. Chem. Soc. Jpn.*, 1988, **61**, 597.
- 11 N. Miyaoura and A. Suzuki, *Chem. Rev.*, 1995, **95**, 2457.
- 12 Y. Miura, H. Oka and M. Momoki, *Synthesis*, 1995, 1419.
- 13 P. D. Bartlett, E. P. Benzing and R. E. Pincock, *J. Am. Chem. Soc.*, 1960, **82**, 1762.
- 14 Y. Miura, A. Yamamoto and M. Kinoshita, *Bull. Chem. Soc. Jpn.*, 1981, **54**, 3215.
- 15 L. Benati, P. C. Montevecchi and P. Spagnolo, *J. Chem. Soc., Perkin Trans. I*, 1982, 3049.
- 16 C. Balboni, L. Benati, P. C. Montevecchi and P. Spagnolo, *J. Chem. Soc., Perkin Trans. I*, 1983, 2111.
- 17 *Gaussian 98, Revision A. 7*, M. J. Frisch, G. W. Trucks, H. B. Schlegel, G. E. Scuseria, M. A. Robb, J. R. Cheeseman, V. G. Zakrzewski, J. A. Montgomery, Jr., R. E. Stratmann, J. C. Burant, S. Dapprich, J. M. Millam, A. D. Daniels, K. N. Kudin, M. C. Strain, O. Farkas, J. Tomasi, V. Barone, M. Cossi, R. Cammi, B. Mennucci, C. Pomelli, C. Adamo, S. Clifford, J. Ochterski, G. A. Petersson, P. Y. Ayala, Q. Cui, K. Morokuma, D. K. Malick, A. D. Rabuck, K. Raghavachari, J. B. Foresman, J. Cioslowski, J. V. Ortiz, A. G. Baboul, B. B. Stefanov, G. Liu, A. Liashenko, P. Piskorz, I. Komaromi, R. Gomperts, R. L. Martin, D. J. Fox, T. Keith, M. A. Al-Laham, C. Y. Peng, A. Nanayakkara, C. Gonzalez, M. Challacombe, P. M. W. Gill, B. Johnson, W. Chen, M. W. Wong, J. L. Andres, M. Head-Gordon, E. S. Replogle and J. A. Pople, Gaussian, Inc., Pittsburgh PA, 1998.
- 18 J. C. Bonner and M. E. Fischer, *Phys. Rev.*, 1964, **A135**, 640.
- 19 (a) W. Duffy, Jr. and K. P. Barry, *Phys. Rev.*, 1968, **165**, 647; (b) J. W. Hall, W. March, R. R. Weller and W. E. Hatfield, *Inorg. Chem.*, 1981, **20**, 1033.
- 20 Y. Miura, M. Momoki, T. Fuchikami, Y. Teki, K. Itoh and H. Mizutani, *J. Org. Chem.*, 1996, **61**, 4300.